Image Reconstruction of a Two-Dimensional Periodic Imperfect Conductor by the Genetic Algorithm

Cheng-Shun Ho and Chien-Ching Chiu
Electrical Engineering Department, Tamkang University, Tamsui, Taipei, R.O.C.
Phone:+886-2-26215656#2615 fax:886-2-26221565
Email: chiu@ee.tku.edu.tw

Abstract - The image reconstruction of a two-dimensional periodic imperfect conductor by the genetic algorithm is investigated. A periodic imperfectly conducting cylinder of unknown periodic length, shape and conductivity scatters the incident wave in free space and the scattered field is recorded outside. Based on the boundary condition and the measured scattered field, a set of nonlinear integral equations is derived and the imaging problem is reformulated into an optimization problem. The genetic algorithm is then employed to find out the global extreme solution of the object function. As a result, the periodic length, the shape and the conductivity of the conductor can be obtained. Numerical results are given to demonstrate that even in the presence of noise, good reconstruction has been obtained.

1. Introduction

The development of inverse scattering techniques for imaging the shape of periodic objects has attracted considerable attention in recent years. There are many important structures whose characteristics are periodic in space. Examples are lattice structure for crystals, photonic band-gap structures and artificial dielectric consisting of periodically placed conducting pieces [1]. Due to its noninvasive nature, inverse scattering can be applied to remote sensing, medical imaging and nondestructive testing. Two main categories of approaches have been developed. The first is an approximate approach, which makes use of the physical optics approximation [2]-[5]. Many papers use the gradient search methods, such as Newton-Kantorovitch method [6]-[8], the local shape function method [9], the Levenberg-Marguart algorithm [10]-[11] and the successive-overrelaxation method [12], to find the solution. However, this method is highly dependent on the initial guess and trends to get trapped in a local extreme. Recently a relative new optimization approach, the genetic algorithm, has been applied to the inverse problem [13]-[15]. Compared to gradient search optimization techniques, the genetic algorithm is less prone to convergence to a local minimum.

To our knowledge, there is still no numerical result for the electromagnetic imaging of periodic scatterers by the above-mentioned rigorous approaches. In this paper, the electromagnetic imaging of a periodic imperfectly conducting cylinder is investigated. The genetic algorithm is used to recover the periodic length, the shape and the conductivity of a scatterer, by using the scattered field. In Section II, the relevant theory and formulations is presented. The general principle of genetic algorithms and the way we applied them to the imaging problem are also described. Numerical simulation is presented to demonstrate the proposed algorithms in Section III. Finally, conclusions are given in Section IV.

II. Theoretical formulation

A periodic two-dimensional imperfectly conducting cylinder with conductivity σ is situated in a background medium with a permittivity ε_o and a permeability μ_o, as shown in Fig. 1.

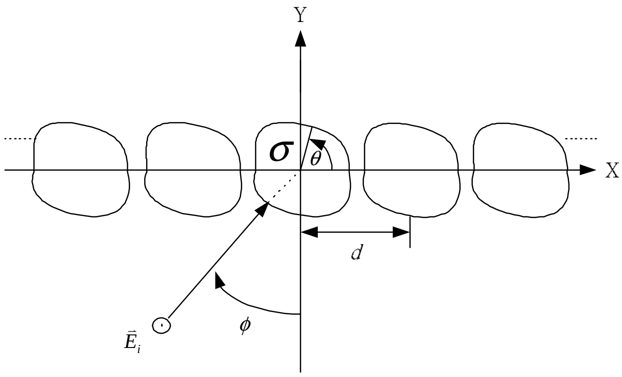

Fig.1 Geometry of a periodic imperfectly conducting cylinder with a periodic spacing *d* along the x-direction.

The array is periodic in the x-direction with a periodic length *d* and is uniform in the z-direction. The cross section of the metallic cylinder is assumed to be described in polar coordinates in xy plane by the equation $\rho=F(\theta)$. A plane wave whose electric field vector is parallel to the z-axis (i.e., transverse magnetic, or TM, polarization) is incident upon the periodic cylinder. Let $\vec{E}_i$ denote the incident wave with incident angel ϕ, as shown in Fig. 1. The scattered field, $\vec{E}_s = E_s\hat{z}$ can be expressed by

$$E_s(x,y) = \int_0^{2\pi} G_l(x,y;x',y')J(\theta')d\theta' \qquad (1)$$

where

$$G_l(x,y;x',y') = \sum_{l=-\infty}^{\infty}\frac{1}{2\alpha_l d}\exp(-\alpha_l|y-y'|)\exp(-jk_l(x-x')) \qquad (2)$$

$$J(\theta) = -j\omega\mu_0\sqrt{F^2(\theta)+F'^2(\theta)}\,J_s(\theta) \qquad (3)$$

with

$$\alpha_l = \begin{cases} j\sqrt{k^2 - k_l^2} & ,k^2 > k_l^2 \\ \sqrt{k_l^2 - k^2} & ,k^2 \le k_l^2 \end{cases} ,$$

$$k_l = \frac{2\pi l}{d} + k\sin\phi\,, \quad k^2 = \omega^2 \varepsilon_0 \mu_0 \tag{4}$$

Here $G_i(x, y; x', y')$ is the two–dimensional periodic Green's function [16], [17], and $J_s(\theta)$ is the induced surface current density which is proportional to the normal derivative of electric field on the conductor surface. The boundary condition for a periodic imperfectly conducting scatterer with finite conductivity can be approximated by assuming that the total tangential electric field on the scatterer surface is related to surface current density through a surface impedance. This boundary condition yields an integral equation for $J(\theta)$:

$$E_i(F(\theta),\theta) = -\int_0^{2\pi} G_i(x, y; x', y') J(\theta') d\theta' + j\sqrt{\frac{j}{\omega\mu_0\sigma}} \frac{J(\theta)}{\sqrt{F^2(\theta) + F'^2(\theta)}} \tag{5}$$

For the direct scattering problem, the scattered field E_s is calculated by assuming that the periodic length *d*, the shape function $F(\theta)$ and the conductivity σ of the object are known. This can be achieved by first solving $J(\theta)$ in (5) and calculating E_s in (1). For numerical calculation of the direct problem, the contour is first divided into sufficient small segments so that the induced surface current can be considered constant over each segment. Then the moment method is used to solve (5) and (1) with pulse basis function for expanding and Dirac delta function for testing. Note that, for numerical implementation of the periodic Green's function, we might face some difficulties in calculating this function. In fact, when y approaches y', the infinite series in (2) is very poor convergent. Fortunately, the infinite series may be rewritten as a rapidly convergent series plus an asymptotic series, which can be summed efficiently. Thus the infinite series in the periodic Green's function can be calculated efficiently [16], [17].

Let us consider the following inverse problem: given the scattered field E_s measured outside the scatterer, determine the periodic length *d*, the shape $F(\theta)$ and the conductivity σ of the object. Assume the approximate center of the scatterer, which in fact can be any point inside the scatter, is known. Then the shape function can be expanded as

$$F(\theta) = \sum_{n=0}^{N/2} B_n \cos(n\theta) + \sum_{n=1}^{N/2} C_n \sin(n\theta) \tag{6}$$

where B_n and C_n are real coefficients to be determined, and N+1 is the number of unknowns for shape function. In the inversion procedure, the genetic algorithm is used to maximum the following object function:

$$OBF = \{\frac{1}{M_t} \sum_{m=1}^{M_t} \frac{\left|E_s^{\exp}(\vec{r}_m) - E_s^{cal}(\vec{r}_m)\right|^2}{\left|E_s^{\exp}(\vec{r}_m)\right|^2} + \alpha\left|F'(\theta)\right|^2\}^{-1/2} \tag{7}$$

where M_t is the total number of measurement points. $E_s^{\exp}(\vec{r}_m)$ and $E_s^{cal}(\vec{r}_m)$ are the measured scattered field and calculated scattered field, respectively. Note that the regularization term $\alpha\left|F'(\theta)\right|^2$ was added in (7). Please refer the reference [11] for detail.

Genetic algorithms are the global numerical optimization methods based on genetic recombination and evolution in nature [28]. They use the iterative optimization procedures that start with a randomly selected population of potential solutions, and then gradually evolve toward a better solution through the application of the genetic operators: reproduction, crossover and mutation operators. In our problem, both parameters *d*, B_n (or C_n) and σ are coded by the following equations:

$$d = p_{\min} + \frac{p_{\max} - p_{\min}}{2^{M_I} - 1} \sum_{i=0}^{M_I - 1} b_i 2^i \tag{8}$$

$$B_n(or\ C_n) = q_{\min} + \frac{q_{\max} - q_{\min}}{2^L - 1} \sum_{i=0}^{L-1} e_i^{B_n(or\ C_n)} 2^i \tag{9}$$

$$\sigma = R_{\min} + \frac{R_{\max} - R_{\min}}{2^{N_I} - 1} \sum_{i=0}^{N_I - 1} f_i 2^i \tag{10}$$

The b_0, b_1, …, $b_{M_I - 1}$ is the M_I-bit string of the binary representation of *d*, and $p_{\min}$ and $p_{\max}$ are the minimum and maximum value admissible for *d*, respectively. Similarly, the $e_0^{B_n(orC_n)}$, $e_1^{B_n(orC_n)}$, …, $e_{L-1}^{B_n(orC_n)}$ (gene) is the L-bit string of the binary representation of B_n (or C_n), and $q_{\min}$ and $q_{\max}$ are the minimum and the maximum values admissible for B_n (or C_n), respectively. Similarly, The f_0, f_1, …, $f_{N_I - 1}$ is the N_I-bit string of the binary representation of σ, and $R_{\min}$ and $R_{\max}$ are the minimum and maximum value admissible for σ, respectively. Here, $p_{\min}$, $p_{\max}$, $q_{\min}$, $q_{\max}$, $R_{\min}$ and $R_{\max}$ can be determined by prior knowledge of the object. Also, the finite resolution with which *d*, B_n (or C_n) and σ can be tuned in practice is reflected in the number of bits assigned to it. The total unknown coefficients in (8)-(10) would then be described by a $M_I + (N+1) \times L + N_I$ bit string (chromosome). The basic GA starts with a large population containing a total of M candidates. A chromosome describes each candidate. Then the initial population can simply be created by taking M random chromosomes. Finally, the GA iteratively generates a new population, which is derived from the previous population through the application of the reproduction, crossover, and mutation operators.

The new populations will contain increasingly better chromosomes and will eventually converge to an optimal population that consists of the optimal chromosomes. As soon as the object function (*OBF*) changes by <1% in two successive generations and the number of generation exceeds pre-given one, the algorithm will be terminated and a solution is then obtained.

III. Numerical results

By a numerical simulation, we illustrate the performance of the proposed inversion algorithm and its sensitivity to random error in the scattered field. Let us consider an imperfectly conducting cylinder array with a periodic length *d* in free space and a plane wave of unit amplitude is incident upon the object, as shown in Fig. 1. The frequency of the incident wave is chosen to be 3 GHz; i.e., the wavelength λ is 0.1 m. In the examples, the size of the scatterer is about one third the wavelength, so the frequency is in the resonance range.

In our calculation, four examples are considered. To reconstruct the periodic length, the shape and the conductivity of the cylinder, the object is illuminated by two incident waves with incident angles ϕ =45° and 135°, and the measurement points are taken on two lines with $Y=\pm 2$ m from x= -0.045 to 0.045 m. Each line has nine measurement points. Note that for each incident angle eighteen measurement points at equal spacing are used, and there are totally 36 measurement points in each simulation. The number of unknowns is set to 11 (i.e., N+3=11), to save computing time. The population size is chosen as 250 (i.e., M =250). The binary string length of the periodic length d is set to be 16 bits (i.e., M_I =16). The binary string length of the unknown coefficient, B_n (or C_n) and σ are also set to be 16 bits (i.e., L=16, $N_I=16$). In other words, the bit number of a chromosome is 176 bits. The search range for the unknown periodic length is chosen from 0.05 to 0.1. The search range for the unknown coefficient of the shape function is chosen to be from 0 to 0.1. The search range for the unknown conductivity is chosen to be from 3×10^7 to 7×10^7. The extreme value of the coefficient of the periodic length, the shape function and the conductivity can be determined by the prior knowledge of the objects. The crossover probability p_c and mutation probability p_m are set to be 0.8 and 0.04, respectively. The value of α is chosen to be 0.001.

For example, the shape function is chosen to be $F(\theta) = (0.03 + 0.009 \cos 3\theta + 0.009 \sin 3\theta)$ m with copper material (i.e., $\sigma = 5.8\times 10^7$ s/m) and a periodic length *d*=0.09 m. The reconstructed shape function for the best population member (chromosome) is plotted in Fig. 2(a) with the error shown in Fig. 2(b), while the error for the reconstructed periodic length and the conductivity are also given in Fig. 2(b).

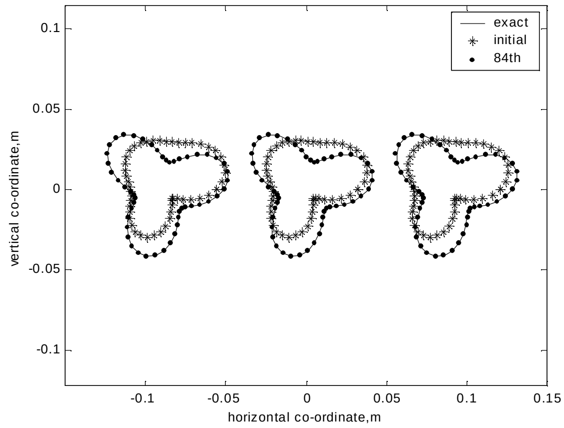

Fig. 2(a) Shape functions for example 1. The solid curve, star curve and dot curve represent the exact shape, initial shape and reconstructed shape, respectively.

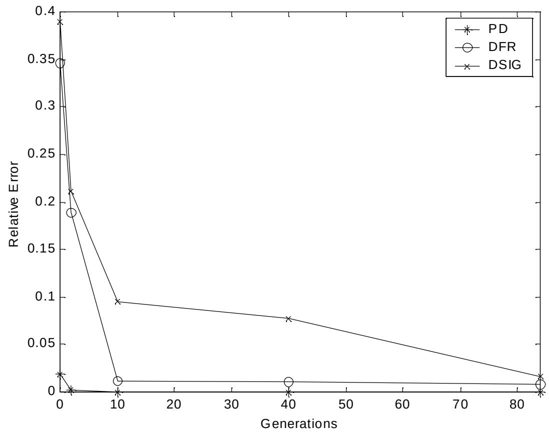

Fig. 2(b) Periodic length error, shape function error and conductivity error in each generation.

Here *PD*, *DFR* and *DSIG* which are called periodic length, shape function and conductivity discrepancies, respectively, are defined as

$$PD = \frac{|d^{cal} - d|}{d} \tag{11}$$

$$DFR = \{\frac{1}{N'}\sum_{i=1}^{N'}[F^{cal}(\theta_i) - F(\theta_i)]^2 / F^2(\theta_i)\}^{1/2} \tag{12}$$

$$DSIG = \frac{|\sigma^{cal} - \sigma|}{\sigma} \tag{13}$$

where N' is set to 100. Quantities *PD*, *DFR* and *DSIG* provide measures of how well d^{cal} approximates *d*, $F^{cal}(\theta)$ approximates $F(\theta)$ and σ^{cal} approximates σ, respectively. From Fig. 3, it is clear that the reconstruction of the periodic length, the shape function and the conductivity is quite good. In addition, we also see that the reconstruction of shape function does not change rapidly toward the exact value until *PD* is small enough and the reconstruction of conductivity does not change rapidly toward the exact value until *PD* and *DFR* are small enough. This can be explained by the fact that the periodic length makes a stronger contribution to the scattered field than the shape function and the conductivity do. Similarly, the shape function makes a stronger contribution to the scattered field than the conductivity does. In other words, the reconstruction of the periodic length has the highest priority and the reconstruction of the conductivity has the lowest priority. To investigate the sensitivity of the imaging algorithm against random noise, two independent Gaussian noises with zero mean have been added to the real and imaginary parts of the simulated scattered fields. Normalized standard deviations of 10^{-5}, 10^{-4}, 10^{-3}, 10^{-2} and 10^{-1} are used in the simulations. The normalized standard deviation mentioned earlier is defined as the standard deviation of the Gaussian noise divided by the rms value of the scattered fields. Here, the signal-to-noise ratio (SNR) is inversely proportional to the normalized standard deviation. The numerical result for this example is plotted in Fig. 3. It is understood that the effect of noise is negligible for normalized standard deviations below 10^{-5}.

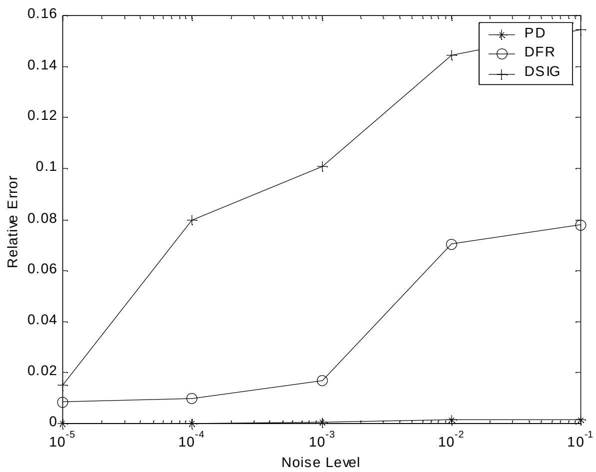

Fig. 3 Relative error of the periodic length, the shape and the conductivity as a function of noise.

IV. Conclusions

We have presented a study of applying the genetic algorithm to reconstruct the periodic length, the shape and the conductivity of a periodic imperfectly conducting cylinder through the knowledge of scattered field. Based on the boundary condition and the measured scattered field, we have derived a set of nonlinear integral equations and reformulated the imaging problem into an optimization one. By using the genetic algorithm, the periodic length, the shape and the conductivity of the object can be reconstructed. Even when the initial guess is far away from exact, the genetic algorithm converges to a global extreme of the object function, while the gradient-based methods often get stuck in a local extreme. Good reconstruction has been obtained from the scattered fields both with and without the additive Gaussian noise. According to our experience, the main difficulties in applying the genetic algorithm to this problem are how to choose the parameters, such as the population size (M), bit length of the string (L), crossover probability (p_c), and mutation probability (p_m). Different parameter sets will affect the speed of convergence as well as the computing time required. From the numerical simulation, it is concluded that a population size from 100 to 300, a string length from 8 to 16 bits, and p_c and p_m in the ranges of 0.7< p_c <0.9 and 0.0005< p_m <0.05 are suitable for imaging problems of this type.

V. References

[1] H. K. Chin, H. C. Chu, and C. H. Chen, "Propagation Modeling of Periodic Laminated Composite Structures", *IEEE Trans. Electromagnetic Compatibility*, vol. 40, pp.218-224, Aug. 1998.

[2] R. M. Lewis, "Physical optics inverse diffraction," *IEEE Trans., Antennas Propagat.*, vol. 17, pp. 308-314, May 1969.

[3] N. N. Bojarski, "A survey of the physical optics inverse scattering identity," *IEEE Trans., Antennas Propagat.*, vol. 30, pp. 980-989, Sept. 1982.

[4] D. B. Ge, "A study of Lewis method for target-shape reconstruction," *Inverse Problems*, vol. 6, pp. 363-370, June 1990.

[5] T. H. Chu and D. B. Lin, "Microwave diversity imaging of perfectly conducting objects in the near-field region," *IEEE Trans. Microwave Theory Tech.*, vol. 39, pp. 480-487, Mar. 1991.

[6] A. Roger, "Newton-Kantorovitch algorithm applied to an electromagnetic inverse problem," *IEEE Trans. Antennas Propagat.*, vol. 29, pp. 232-238, Mar. 1981.

[7] W. Tobocman, "Inverse acoustic wave scattering in two dimensions from impenetrable targets," *Inverse Problems*, vol. 5, pp. 1131-1144, Dec. 1989.

[8] C. C. Chiu and Y. W. Kiang, "Electromagnetic imaging for an imperfectly conducting cylinders," *IEEE Trans. Microwave Theory Tech.*, vol. 39, pp. 1632-1639, Sept. 1991.

[9] G. P. Otto and W. C. Chew, "Microwave inverse scattering-local shape function imaging for improved resolution of strong scatterers," *IEEE Trans. Microwave Theory Tech.*, vol. 42, pp. 137-141, Jan. 1994.

[10] D. Colton and P. Monk, "A novel method for solving the inverse scattering problem for time-harmonic acoustic waves in the resonance region II," SIAM J. *Appl. Math.*, vol. 46, pp. 506-523, June 1986.

[11] F. Hettlich, "Two methods for solving an inverse conductive scattering problem," *Inverse Problems*, vol. 10, pp. 375-385, 1994.

[12] R. E. Kleinman and P. M. van den Berg, "Two-dimensional location and shape reconstruction," *Radio Sci.*, vol. 29, pp.

1157-1169, July- Aug. 1994.

[13] Z. Q. Meng, T. Takenaka and T. Tanaka, “Image reconstruction of two-dimensional impenetrable objects using genetic algorithm,” *Journal of Electromagnetic Waves and Application*, vol. 13, pp. 95- 118, 1999.

[14] A. Qing and C. K. Lee. “Microwave imaging of a perfectly conducting cylinder using a real-coded genetic algorithm,” *IEE Proc.-Microw. Antennas Propag.*, vol. 146, pp. 421-425, December 1999.

[15] C. C. Chiu and W. T. Chen, "Electromagnetic imaging for an imperfectly conducting cylinder by the genetic algorithm," *IEEE Trans. Microwave Theory Tech.*, vol. 48, pp. 1901-1905, Nov. 2000.

[16] R. E. Jorgenson and R. Mittra, “Efficient calculation of free-space periodic Green’s function,” *IEEE Trans. Antenna Propagat.*, vol. 38, pp. 633-642, May 1990.

[17] G. S. Wallinga, E. J. Rothwell, K. M. Chen, and D. P. Nyquist, “Efficient computation of the two-dimensional periodic Green’s function,” *IEEE Tran. Antenna Propagat.*, vol. 47, pp. 895-897, May 1999.

[18] D. E. Goldgerg, *Genetic Algorithm in Search, Optimization and Machine Learning*. Addison-Wesley, 1989.